Int. J. Heat Mass Transfer. Vol. 32, No. 6, pp. 1095–1103, 1989
Printed in Great Britain

0017-9310/89 $3.00+0.00
Pergamon Press plc

Transient natural convection in prismatic enclosures of arbitrary cross-section

YU. E. KARYAKIN

Department of Physical and Mechanical Engineering, Leningrad Polytechnic Institute, Leningrad, 195251, U.S.S.R.

(*Received* 20 *July* 1988)

Abstract—Two-dimensional laminar natural convection in horizontal prismatic enclosures of arbitrary cross-section is investigated. With the Boussinesq approximation the convection equations are written in a curvilinear non-orthogonal coordinate system and are solved by the implicit finite-difference method. Transient natural convection is studied in quadrangular regions of non-conventional configurations: (a) an isosceles trapezium; (b) a portion of a circle confined between two equal and parallel chords; (c) a region with the boundaries formed by the cosine semi-wave and three segments of straight lines. The solution of the problems is obtained within the range of Grashof numbers $10^2 \leqslant Gr \leqslant 10^6$ at different geometrical parameters of the enclosures. It is found that the maximum values of the stream function and Nusselt number may accomplish damping oscillations about their stationary values. The results obtained for the trapezoidal enclosures are in good agreement with the data reported by other authors.

1. INTRODUCTION

IN RECENT years there has been a marked upsurge of interest shown in the numerical study of natural convection within enclosed cavities. The successes achieved in the so-called numerical experiment have become possible due to the development of effective methods for solving the Navier–Stokes equations and to the use of large-capacity computers.

The overwhelming majority of works dealing with convection in enclosures is restricted to the cases of comparatively simple geometry: rectangular, cylindrical and spherical cavities [1–3]. The configuration of actual containers occurring in practice is often far from being simple. The investigation in unconventional enclosures can be found in refs. [4–14].

Convective motion of a fluid in rectangular enclosures with protrusions, partitions or fins is investigated in refs. [4, 5]. It is noted that a mean heat flux through an enclosure decreases with an increase in fin size.

Quite frequently the channels of building constructions, panels of electronic equipment, current leads in the electrotechnical industry, and solar energy collectors have the shape of triangular prisms. Numerical simulation of convective processes in such enclosures is performed in refs. [6–8].

Reference [9] considers two-dimensional natural convection in a parallelogram-shaped enclosure. The vertical walls are assumed to be isothermal (cold and hot), while the linear temperature distribution or the condition of thermal insulation is given on the other two parallel walls. The results of calculations are compared with the experimental data. In ref. [10] the same problem is solved in a conjugated formulation.

Convection in a region formed by concentric circular arcs and radial straight lines is considered in refs. [11, 12]. The computational study of convection in a trapezoidal enclosure with thermally insulated bases and isothermal walls inclined at an angle of 45° is made in ref. [13]. The solution of the problem is obtained with the use of stream function–vorticity variables in the range $10^2 \leqslant Ra \leqslant 10^5$ at different enclosure orientations with respect to the gravity vector.

Finally, ref. [14] deals with laminar and turbulent natural convection in a complex geometry region. Based on elliptic equations, the generation of a body-fitted numerical grid is fulfilled. The problem is solved with the use of stream function–vorticity variables. Turbulent modes of flow are considered with the aid of the two-parametric model of turbulence. As an example, natural convection in a region with sinusoidal boundaries is considered.

Numerical simulation of natural convection heat transfer in arbitrary shaped regions imposes special requirements on the coordinate system of the problem. There are several ways for selecting the system. First, it is possible to use a Cartesian rectangular coordinate system. However, since it is necessary that boundary conditions be specified at irregular grid points with a corresponding loss in solution accuracy, it is impossible to generate body-fitted numerical grids, and this makes the system of little value. Second, in some cases the use of mixed grids is possible (e.g. rectangular Cartesian grids over linear segments of the region and polar ones over the sectors of a circle, etc.). It goes without saying that not every configuration admits this approach. Moreover, some difficulties arise with matching solutions at the boundaries of subregions where the Jacobi matrix coefficients may be discontinuous.

NOMENCLATURE

c_p coefficient of heat capacity
d_{1i}, d_{2i} grid thickening coefficients
g free fall acceleration
g_i covariant g-components
g^{kl} metric tensor components
Gr Grashof number, $\beta g(T_1 - T_2)L^3/\nu^2$
H height of cavity
h_1, h_2 heights of side walls
L characteristic length
Nu local Nusselt number, $(\partial\theta/\partial n)_w$
$\overline{Nu}$ mean Nusselt number
p pressure
Pr Prandtl number, $\rho\nu c_p/\lambda$
R radius
Ra Rayleigh number, $Gr\,Pr$
T_1, T_2 dimensional characteristic temperatures
t time
u_1, u_2 Cartesian velocities
v_1, v_2 covariant velocity vector components
v^1, v^2 contravariant velocity vector components
x^1, x^2 curvilinear coordinates
y_1, y_2 Cartesian coordinates
z_i auxiliary variables.

Greek symbols
β thermal coefficient of volumetric expansion
Δ increment of a quantity
δ correction to the sought-after quantity
θ relative temperature
λ coefficient of thermal conductivity
ν kinematic viscosity
ρ density
τ relaxation time
ϕ angle of inclination
ψ stream function.

Subscripts
max maximum value
Q at the differentiation point Q
w on the wall
y_i projection on the Cartesian y_i-axis
0 scale of the quantity.

The most effective system, which would be free from the aforementioned shortcomings, is regarded to have coordinate lines (or surfaces) which coincide with the boundaries of the region. In a general case this system will be curvilinear and non-orthogonal.

This paper considers numerical simulation of transient natural convection within regions of arbitrary configuration on the basis of Navier–Stokes and energy equations written in the curvilinear non-orthogonal coordinate system. The specific features of the solution of such problems can be found elsewhere [15].

2. MATHEMATICAL FORMULATION

Consider a horizontal prismatic container of large extension the cross-section of which (a quadrangle ABCD with arbitrary curvilinear boundaries) is depicted in Fig. 1. The gravity vector is located in the plane of this cross-section.

It will be assumed that in the region ABCD under study a laminar natural convection occurs with moderate temperature variations for which the Boussinesq approximation is valid. The heat generation due to viscous dissipation and the work of compression forces are neglected.

With the above assumptions, the governing equations of two-dimensional unsteady-state natural convection can be written in the Cartesian coordinate system (y_1, y_2) as

$$\frac{\partial u_i}{\partial t} + \frac{\partial}{\partial y_k}(u_k u_i) = -Gr\frac{g_{y_i}}{g}\theta - \frac{\partial p}{\partial y_i} + \frac{\partial}{\partial y_k}\left(\frac{\partial u_i}{\partial y_k}\right) \quad (1)$$

$$\frac{\partial \theta}{\partial t} + \frac{\partial}{\partial y_k}(u_k\theta) = \frac{1}{Pr}\frac{\partial}{\partial y_k}\left(\frac{\partial \theta}{\partial y_k}\right) \quad (2)$$

$$\frac{\partial u_k}{\partial y_k} = 0, \quad i = 1,2; \quad k = 1,2. \quad (3)$$

Here and hereafter, repeated indices imply the summation from 1 to 2.

Equations (1)–(3) are presented in dimensionless form. The linear scale is selected to be the charac-

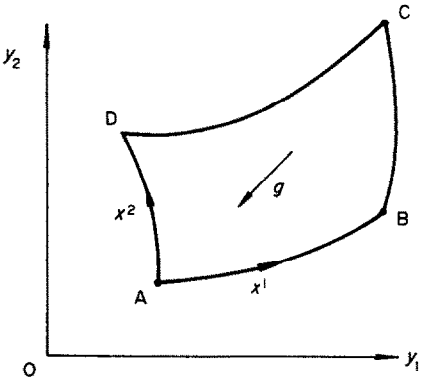

FIG. 1. The plane of Cartesian (y_1, y_2) and curvilinear (x^1, x^2) coordinates.

teristic length L, the time scale is taken to be the diffusion time $t_0 = L^2/\nu$, the velocity scale will be the quantity $u_0 = L/t_0 = \nu/L$, and the pressure scale is taken to be twice the dynamic head $\rho u_0^2 = \rho\nu^2/L^2$.

Let (x^1, x^2) be the curvilinear non-orthogonal coordinate system in the plane of the cross-section ABCD the coordinate lines of which coincide with the boundaries of the region. Now impose the requirement that the transformations $x^1 = x^1(y_1, y_2)$ and $x^2 = x^2(y_1, y_2)$ map the investigated region on the canonical region, i.e. a unit square ($0 \leqslant x^1 \leqslant 1$, $0 \leqslant x^2 \leqslant 1$).

In the coordinate system (x^1, x^2) equations (1)–(3) have the following tensor form [15]:

$$\frac{\partial v_l}{\partial t} + \nabla_k(v^k v_l) = -Gr\frac{g_l}{g}\theta - \nabla_l p + g^{kl}\nabla_k(\nabla_l v_i) \tag{4}$$

$$\frac{\partial \theta}{\partial t} + \nabla_k(v^k\theta) = \frac{1}{Pr}g^{kl}\nabla_k(\nabla_l\theta) \tag{5}$$

$$g^{kl}\nabla_k v_l = 0, \quad i,k,l = 1,2 \tag{6}$$

where

$$g^{kl} = \frac{\partial x^k}{\partial y_\alpha}\frac{\partial x^l}{\partial y_\alpha}. \tag{7}$$

The covariant, v_i, and contravariant, v^i, velocity vector components are associated with the Cartesian components u_α by means of the familiar relationships of tensor analysis [16]

$$v_i = u_\alpha\frac{\partial y_\alpha}{\partial x^i}, \quad v^i = u_\alpha\frac{\partial x^i}{\partial y_\alpha}, \quad u_\alpha = v_i\frac{\partial x^i}{\partial y_\alpha} = v^i\frac{\partial y_\alpha}{\partial x^i},$$
$$i,\alpha = 1,2. \tag{8}$$

Expressions analogous to equations (8) may be written for tensor components of any rank in transition from the Cartesian (y_1, y_2) to the arbitrary curvilinear (x^1, x^2) coordinate system. These expressions can be used to transform equations (4)–(6) to a form without tensor derivatives.

Thus, using expressions (A1)–(A5) (see Appendix), it is possible to replace equations (4)–(6) by the following system of equations which describe transient natural convection in an arbitrary non-orthogonal coordinate system:

$$\frac{\partial v_i}{\partial t} + \frac{\partial(\hat{v}^k\hat{v}_i)}{\partial x^k} = -Gr\frac{g_i}{g}\theta - \frac{\partial p}{\partial x^i} + \frac{\partial}{\partial x^k}\left(\hat{g}^{kl}\frac{\partial\hat{v}_i}{\partial x^l}\right) \tag{9}$$

$$\frac{\partial\theta}{\partial t} + \frac{\partial(\hat{v}^k\theta)}{\partial x^k} = \frac{1}{Pr}\frac{\partial}{\partial x^k}\left(\hat{g}^{kl}\frac{\partial\theta}{\partial x^l}\right) \tag{10}$$

$$\frac{\partial}{\partial x^k}(\hat{g}^{kl}v_l) = 0, \quad i,k,l = 1,2. \tag{11}$$

The symbol ($\hat{}$) denotes the quantities calculated with the help of the derivatives $\partial x^i/\partial y_\alpha$ and $\partial y_\alpha/\partial x^i$ fixed at the differentiation point Q

$$\hat{v}_i = u_\alpha\left(\frac{\partial y_\alpha}{\partial x^i}\right)_Q = v_k\frac{\partial x^k}{\partial y_\alpha}\left(\frac{\partial y_\alpha}{\partial x^i}\right)_Q = v_k\hat{g}_i^k \tag{12}$$

$$\hat{v}_k = u_\alpha\left(\frac{\partial x^k}{\partial y_i}\right)_Q = v_l\frac{\partial x^l}{\partial y_\alpha}\left(\frac{\partial x^k}{\partial y_\alpha}\right)_Q = v_i\hat{g}^{kl} \tag{13}$$

$$\hat{g}_i^k = \frac{\partial x^k}{\partial y_\alpha}\left(\frac{\partial y_\alpha}{\partial x^i}\right)_Q, \quad \hat{g}^{kl} = \frac{\partial x^l}{\partial y_\alpha}\left(\frac{\partial x^k}{\partial y_\alpha}\right)_Q. \tag{14}$$

The system of equations (9)–(11) is augmented with the corresponding conditions on all the solid boundaries of the region: the non-slip and non-flow conditions for the velocity vector components, first- and second-kind boundary conditions for the temperature θ.

Since in physical variables the pressure p is determined from equations (9) accurate to an arbitrary constant, an additional condition is used, e.g. $p = 0$ at the point $x^1 = x^2 = 0$. No other boundary conditions are used for the pressure.

In the case of unsteady-state processes, initial conditions should also be given. When solving actual problems, it is supposed that at the initial time instant the fluid is quiescent throughout the entire convection region and that its temperature is everywhere equal to $\theta_0 = 0.5$.

3. METHOD OF SOLUTION

When constructing the finite-difference scheme for solving equations (9)–(11), a non-uniform grid with exponential thickening near the solid boundaries is used. For this purpose, the auxiliary variables z_i ($i = 1,2$) are introduced which vary with a constant grid step Δz_i and which are associated with the coordinates x^i ($i = 1,2$) by

$$z_i = \frac{1}{2}\left\{1 + \frac{\ln(1+d_{1i}x^i)}{\ln(1+d_{1i})} - \frac{\ln[1+d_{2i}(1-x^i)]}{\ln(1+d_{2i})}\right\}$$

where $0 \leqslant z_1 \leqslant 1$, $0 \leqslant z_2 \leqslant 1$. The grid thickening coefficients were supposed to be equal to $d_{1i} = d_{2i} = 10$.

The unknown grid functions v_1, v_2, p and θ are determined at the points of grid cells which are shifted relative to one another, as is conventional in the MAC method [17]. The pressure p and temperature θ are specified in the centre of each cell, the function v_1 in the middle of its left- and right-hand sides and the function v_2 in the middle of the upper and lower bases of the cell. The convective terms in equations (9)–(11) are approximated according to the donor-cell method, whereas the remaining terms are approximated with conventional central differences.

The resulting finite-difference equations are solved for the corrections δv_1, δv_2, δp and $\delta\theta$ to the unknown quantities with the aid of an implicit multi-step scheme [15] and thorough optimization of its individual stages.

To find the field of the function δp, continuity equation (11) is supplemented with the relaxation time derivative $\partial(\delta p)/\partial\tau$, then it is split along the x^1- and x^2-axes and is solved by using the standard tri-diagonal

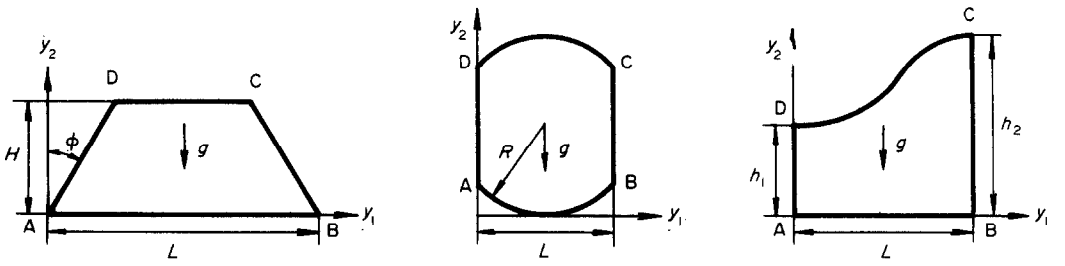

FIG. 2. Configurations of convection regions.

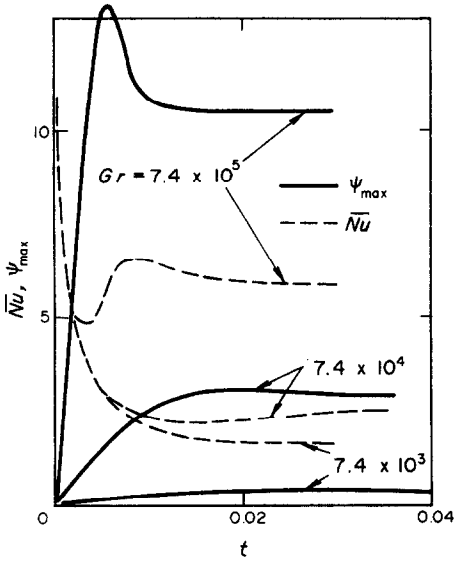

FIG. 3. The functions $\psi_{max}(t)$ and $\overline{Nu}(t)$ in a trapezoidal enclosure.

metric algorithm. To speed up the convergence of the iterative process, the set of relaxation time steps is used $\Delta\tau \{\Delta\tau_0, \Delta\tau_1, \ldots, \Delta\tau_\kappa\}$, which ensures a uniform damping of the error in the whole spectrum of the problem eigenvalues [18]. Note that the finite-difference equation for the correction δp does not require any additional boundary conditions. In the vicinity of the convection region boundary, the finite-difference analogues for partial differential operators are written in a form which takes into account only the boundary conditions for the velocity vector components and temperature.

The implicit solution of equations (9) and (10) is carried out by analogous schemes using the method of oriented splitting [15]. The character of splitting is determined by the flow direction and is carried out directly in the course of problem solution. The resulting finite-difference scheme acquires a parabolic character, it is especially effective in the investigation of fluid motions with circulation zones.

When the second-kind temperature boundary condition is specified at any of the enclosure walls, then it is necessary to take into consideration that (no summation over i)

$$\left.\frac{\partial\theta}{\partial n}\right|_{x^i=\text{const.}} = \frac{1}{\sqrt{g^{ii}}}\left(g^{1i}\frac{\partial\theta}{\partial x^1} + g^{2i}\frac{\partial\theta}{\partial x^2}\right), \quad i = 1, 2$$

where n is a normal to the coordinate line $x^i = \text{const.}$ Since the derivative $\partial\theta/\partial n$ simultaneously contains the derivatives $\partial\theta/\partial x^1$ and $\partial\theta/\partial x^2$, then its finite-difference analogue can be realized with the help of the factorization method along the boundary where this condition is given.

All the calculations were made on a non-uniform 30×30 grid.

4. RESULTS OF COMPUTATIONS

The above-described procedure was applied to numerical simulation of natural convection in regions of several configurations. In all the cases it was assumed that $Pr = 0.7$ and that the gravity vector was parallel to the $0y_2$-axis.

It will be adopted that the upper and lower bases of the enclosure are insulated and that the side walls are isothermal (hot and cold)

$$\theta_{AD} = 1, \quad \theta_{BC} = 0, \quad \left.\frac{\partial\theta}{\partial n}\right|_{AB} = \left.\frac{\partial\theta}{\partial n}\right|_{DC} = 0. \quad (15)$$

The calculations were carried out within the range $10^2 \leqslant Gr \leqslant 10^6$. The developments in time of stream lines, isotherms and maximum values of the stream function were constructed, determined in the section $x^1 = \text{const.}$ as

$$\psi = \int_0^{x^2} \sqrt{\left(\frac{g_{22}}{g^{11}}\right)}(v_1 g^{11} + v_2 g^{21})\, dx^2 \quad (16)$$

as well as the distribution of the local Nusselt number on the side walls of the enclosure.

4.1. *Isosceles trapezium*

Consider natural convection in a two-dimensional cavity bounded by an isosceles trapezium (Fig. 2(a)) of height H and with the base of length L. The side walls form an angle ϕ with the vertical.

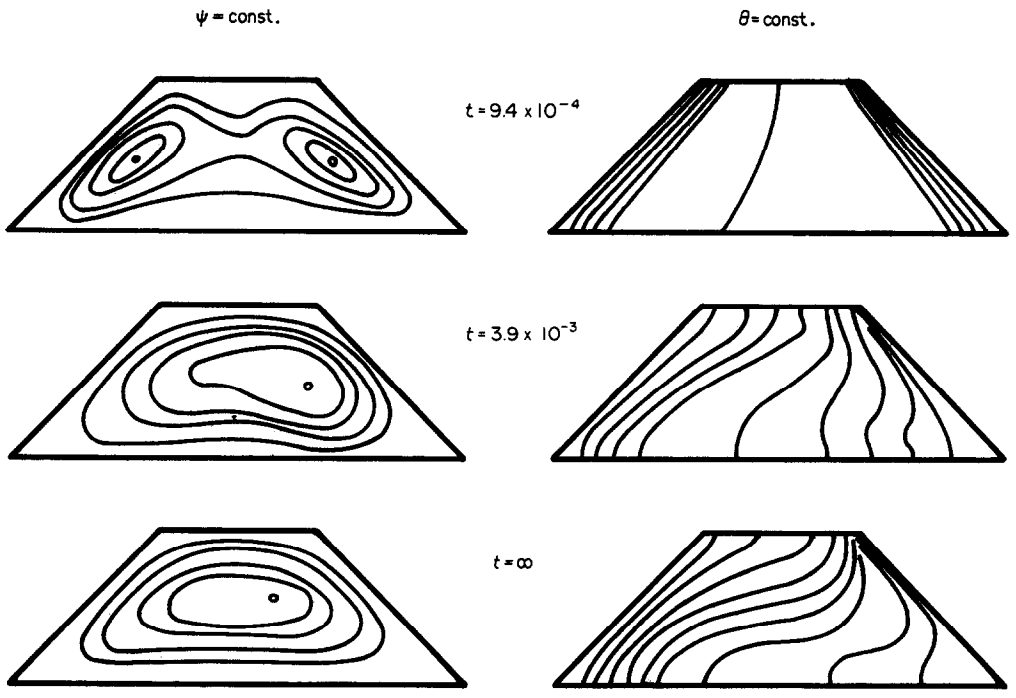

FIG. 4. Stream lines and isotherms in a trapezoidal enclosure.

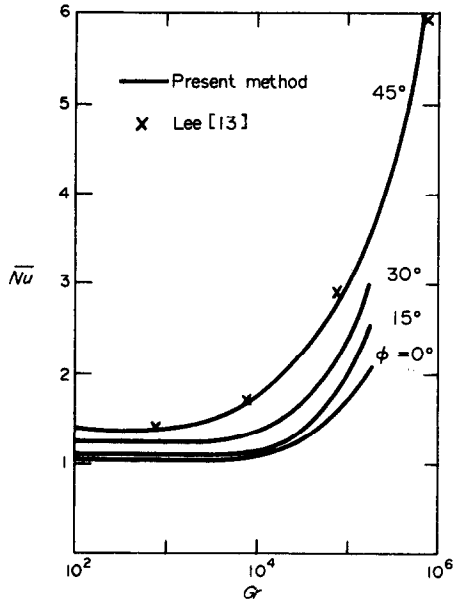

FIG. 5. The influence of the angle ϕ on the function $\overline{Nu}(Gr)$ in a trapezoidal enclosure.

The curvilinear coordinate system (x^1, x^2) will be introduced as follows:

$$x^1 = \frac{y_1 - y_2 \tan\phi}{L - 2y_2 \tan\phi}, \quad x^2 = \frac{y_2}{H}. \tag{17}$$

In this case, the trapezoidal region of motion ABCD on the coordinate plane (y_1, y_2) transforms into a quadratic one on the plane (x^1, x^2), so that $0 \leqslant x^1 \leqslant 1$ and $0 \leqslant x^2 \leqslant 1$, and its boundaries coincide with the coordinate lines $x^1 = \text{const.}$ and $x^2 = \text{const.}$

Using expressions (17) and the inverse coordinate transformations, one can easily find the values of the Jacobi matrix elements $\partial y_\alpha/\partial x^i$ and $\partial x^i/\partial y_\alpha$ $(i, \alpha = 1, 2)$ necessary for calculations. Henceforth it will be assumed that $L = 1$ and $H = L/3$.

The solid lines in Fig. 3 show the change with time of the maximum value of the stream function in an enclosure for the case of $\phi = 45°$ and three Grashof numbers: 7.4×10^3, 7.4×10^4 and 7.4×10^5 (taking into consideration the difference in the choice of scales, this corresponds to $Ra = 10^3$, 10^4 and 10^5 in ref. [13]). The dashed lines in the same figure show the mean Nusselt numbers at the side wall.

At comparatively small Grashof numbers, $Gr \leqslant 10^4$, the maximum value of the stream function, which characterizes the intensity of convection motion, increases monotonously with time, approaching a certain limit. The local Nu are great at the beginning of the process because of high temperature gradients near the walls, then they decrease monotonously with time, tending to a certain limit.

When $Gr > 10^4$, the functions $\psi_{max}(t)$ and $\overline{Nu}(t)$ are no longer monotonous. At a certain time instant the quantity ψ_{max} attains a maximum and then, decreases, tending to a steady-state value. The non-monotonous behaviour of the functions $\psi_{max}(t)$ and $\overline{Nu}(t)$ is also typical for cavities of other shapes. Thus, an anal-

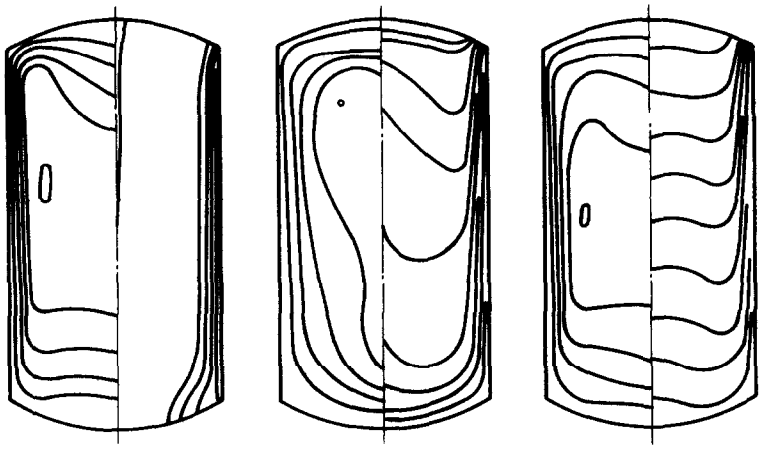

FIG. 6. Stream lines and isotherms in the cavity formed by a part of a circle.

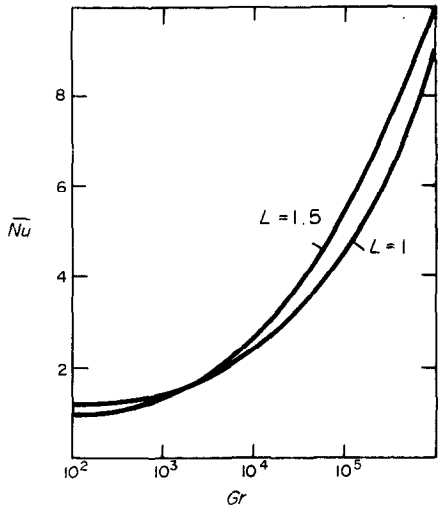

FIG. 7. The influence of the width L on the function $\overline{Nu}(Gr)$ for the cavity formed by a part of a circle.

ogous phenomenon is described in ref. [8] for a triangular enclosure.

The change with time of the stream lines and isotherms in the cavity for the case of $Gr = 7.4 \times 10^5$ and $\phi = 45°$ is shown in Fig. 4. The stream lines are presented with the step $\Delta\psi/\psi_{max} = 0.2$, and the isotherms with the step $\Delta\psi/\psi_{max} = 0.1$. As follows from Fig. 4, at the beginning of convection two circulation zones are formed near the side walls, with clockwise rotation of the fluid. As time goes on, these zones merge into a single circulation region. In the central part of the enclosure the isotherms acquire almost a horizontal position which corresponds to the conditions of fluid stratification.

In Fig. 5 the function $\overline{Nu}(Gr)$ is given for different angles ϕ of side wall inclination. The data of ref. [13] designated as crosses are given for comparison. The coincidence between the results should be regarded as satisfactory. As is seen, the rate of heat transfer processes on the side walls of the enclosure increases noticeably with the angle ϕ.

4.2. *A part of a circle*

Now consider natural convection in a horizontal cylindrical enclosure the cross-section of which is a part of a circle with radius R disposed between two equal and parallel chords at a distance L form one another (Fig. 2(b)). The curvilinear coordinate system (x^1, x^2) will be introduced in the following manner:

$$x^1 = \frac{1}{L}\left(y_1 - R + \frac{L}{2}\right)$$

$$x^2 = \frac{y_2 - R + \sqrt{(R^2 - L^2(x^1 - 0.5)^2)}}{2\sqrt{(R^2 - L^2(x^1 - 0.5)^2)}}. \quad (18)$$

The governing convection equations (9)–(11) with boundary conditions (15) provide the central symmetry of solution in the case when the gravity vector is parallel to the side walls of the enclosure. Then

$$\begin{aligned} v_1(x^1, x^2) &= -v_1(1-x^1, 1-x^2) \\ v_2(x^1, x^2) &= -v_2(1-x^1, 1-x^2) \\ p(x^1, x^2) &= p(1-x^1, 1-x^2) - (1-x^2)Gr \\ \theta(x^1, x^2) &= 1 - \theta(1-x^1, 1-x^2). \end{aligned} \quad (19)$$

However, when applying the difference algorithm, conditions (19) are not used. To control the accuracy of results, the problem is solved for the entire convection region ABCD.

The calculations were made for $R = 1$ and two widths of the enclosure: $L = 1$ and 1.5. When $Gr \geqslant 10^5$, the functions $\psi_{max}(t)$ and $\overline{Nu}(t)$ tend to stationary values accomplishing a sort of damping oscillation.

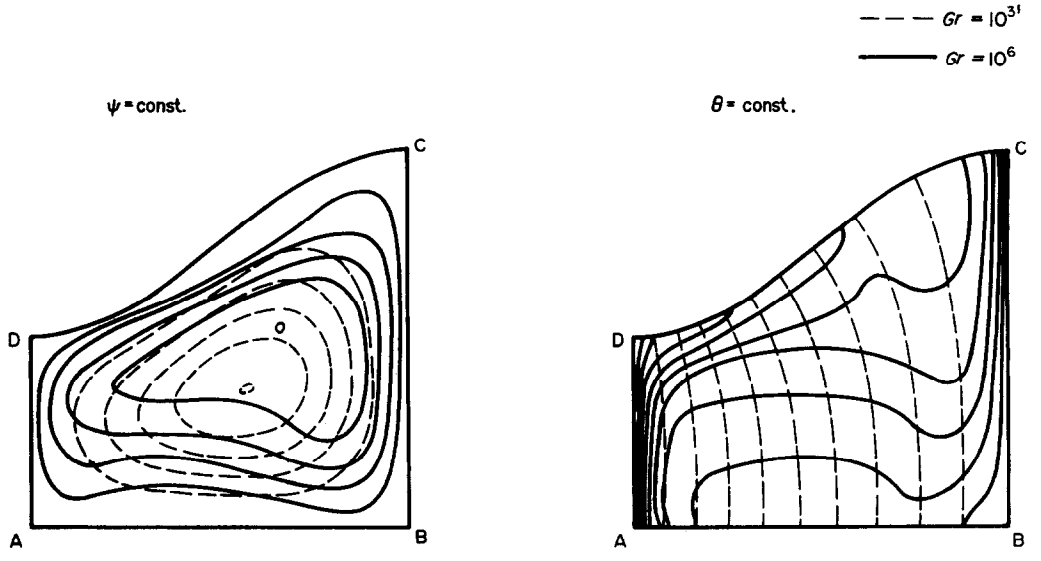

FIG. 8. Stream lines and isotherms in the cavity with a cosinusoidal boundary.

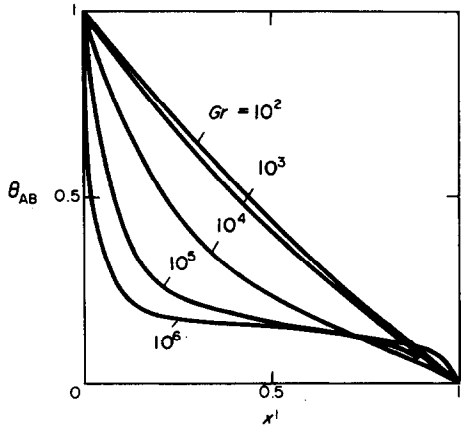

FIG. 9. Temperature distribution on the lower wall of the cavity with a cosinusoidal boundary.

The change with time of the transient convection process in the cavity at $L = 1$ and $Gr = 10^6$ is shown in Fig. 6. In the central part of the enclosure the isotherms shift from the vertical into the horizontal position which corresponds to the conditions of fluid stratification. Gradient regions appear on the solid walls which resemble dynamic and temperature boundary layers.

In Fig. 7 the variation of the mean Nusselt number with Grashof number is given for two types of enclosures: with $L = 1$ and 1.5. At small Grashof numbers ($Gr \leqslant 10^3$) the processes which take place in the enclosure are mainly determined by heat conduction. In the steady-state convection regime, the isotherms are almost vertical, the greater number $\overline{Nu}$ corresponds to the smaller distance L between the side walls. At large Gr, the convection processes taking place in the enclosure dominate fully over heat conduction. The growth of the distance L between the side walls promotes the involvement of the greater portion of fluid into the main circulation motion and its better mixing, and this leads to the growth of $\overline{Nu}$.

4.3. *A region with a cosinusoidal boundary*

At last, consider natural convection in a cylindrical enclosure the cross-section of which is formed by three segments of straight lines and by the cosine semi-wave (Fig. 2(c)). If L is the width of the enclosure base, h_1 and h_2 are the heights of the left- and right-hand side wall, respectively, then the curvilinear system of coordinates (x^1, x^2) can be introduced as follows:

$$x^1 = \frac{y_1}{L}, \quad x^2 = \frac{2y_2}{h_1 + h_2 - (h_2 - h_1)\cos(\pi x^1)}. \tag{20}$$

The calculations were made for $L = 1$, $h_1 = 0.5$ and $h_2 = 1$. In Fig. 8(a) the stream lines in the developed convective regime are given with the step $\Delta\psi/\psi_{max} = 0.2$. The dashed lines characterize the case of $Gr = 10^2$, the solid lines the case with $Gr = 10^6$. The isotherms corresponding to these cases are given in Fig. 8(b) with the step $\Delta\theta = 0.1$. As Gr increases, the intensity of convective processes grows, and pronounced temperature boundary layer regions are formed on the side walls. In the central part of the enclosure, the isotherms shift from the vertical into the horizontal position. Figure 9 shows the distribution of the temperature θ along the enclosure base AB at different Grashof numbers in the steady-state convection regime.

When at $Gr = 10^2$ the distribution is close to linear, then at $Gr = 10^6$ the temperature is practically constant over the greatest portion of the insulated base, and only near the side wall the temperature gradients are appreciable.

5. CONCLUSIONS

(1) The system of differential equations describing the unsteady-state natural convection under the Boussinesq approximation is obtained in an arbitrary curvilinear non-orthogonal coordinate system. The covariant velocity vector components, pressure and temperature are used as dependent variables.

(2) The implicit multi-step finite-difference method of solving the natural convection equations in an arbitrary enclosure is used with the splitting oriented with respect to the fluid flow and with the optimization of all its individual stages.

(3) Transient natural convection in three types of two-dimensional enclosures is numerically simulated: trapezoidal region, a portion of a circle and a region with a cosinusoidal boundary.

(4) The range of Grashof numbers $10^2 \leqslant Gr \leqslant 10^6$ is studied at different values of the geometrical parameters of the enclosure. The temperature boundary conditions correspond to the side heating and insulation of the base.

(5) The steady-state convection regime at large Gr is achieved nonmonotonically.

(6) With the growth of Gr, the isotherms in the central part of the enclosure shift into a horizontal position which corresponds to conditions of fluid stratification. At large Gr on the side walls, there appear gradient regions which resemble dynamic and temperature boundary layers.

REFERENCES

1. G. Z. Gershuni, E. M. Zhukhovitsky and E. L. Tarunin, Numerical investigation of convection motion in an enclosed cavity, *Izv. Akad. Nauk SSSR, Mekh. Zhidk. Gaza* No. 5, 56–62 (1966).
2. I. P. Jones and C. P. Thompson (Editors), Numerical solutions for a comparison problem on natural convection in an enclosed cavity, AERE-R9955, Harwell (1981).
3. O. G. Martynenko and Yu. A. Sokovishin, *Free-convective Heat and Mass Transfer (Bibliography)*, Parts 1, 3 and 4. ITMO AN BSSR, Minsk (1982, 1987).
4. G. B. Petrazhitskiy, F. V. Klyushnikov and E. V. Bekneva, The influence of the enclosure shape on the natural convection heat transfer rate, *Trudy MVTU* No. 195, vyp. 2, 56–70 (1975).
5. Yu. E. Karyakin, O. G. Martynenko and Yu. A. Sokovishin, Free convection in a rectangular enclosure with side fins, Preprint No. 22 of the Heat and Mass Transfer Institute, Minsk (1984).
6. V. A. Akinsete and T. A. Coleman, Heat transfer by steady laminar free convection in triangular enclosures, *Int. J. Heat Mass Transfer* **25**, 991–998 (1982).
7. Yu. E. Karyakin and Yu. A. Sokovishin, Unsteady-state natural convection in a triangular enclosure, *Izv. Akad. Nauk SSSR, Mekh. Zhidk. Gaza* No. 5, 169–173 (1985).
8. Yu. E. Karyakin, O. G. Martynenko, Yu. A. Sokovishin and Kh. Z. Ustok, Numerical simulation of unsteady-state natural convection in triangular enclosures, *Heat Transfer—Sov. Res.* **17**(3), 1–33 (1985).
9. H. Nakamura and Y. Asako, Heat transfer in a parallelogram shaped enclosure, *Bull. J.S.M.E.* **23**, 1827–1834 (1980).
10. Y. Asako and H. Nakamura, Heat transfer in a parallelogram shaped enclosure, *Bull. J.S.M.E.* **27**, 1144–1151 (1984).
11. L. Iyican, Y. Bayazitoglu and L. C. Witte, An analytical study of natural convective heat transfer within a trapezoidal enclosure, *J. Heat Transfer* **102**, 640–647 (1980).
12. L. Iyican, L. C. Witte and Y. Bayazitoglu, An experimental study of natural convection in trapezoidal enclosures, *J. Heat Transfer* **102**, 648–653 (1980).
13. T. S. Lee, Computational and experimental studies of convective fluid motion and heat transfer in inclined non-rectangular enclosures, *Int. J. Heat Fluid Flow* **5**, 29–36 (1984).
14. J. P. Coulter and S. I. Güceri, Laminar and turbulent natural convection within irregularly shaped enclosures, *Numer. Heat Transfer* **12**, 211–227 (1987).
15. O. G. Martynenko, Yu. A. Sokovishin and Yu. E. Karyakin, Free convection on a vertical surface and in regions of arbitrary configuration, Preprint No. 3 of the Heat and Mass Transfer Institute, Minsk (1988).
16. G. A. Korn and T. M. Korn, *Mathematical Handbook for Scientists and Engineers*. McGraw-Hill, New York (1961).
17. P. J. Roache, *Computational Fluids Dynamics*. Hermosa, Albuquerque (1976).
18. V. E. Karyakin and Yu. E. Karyakin, Calculation of viscous fluid flows in two-dimensional channels of arbitrary configuration, *Chisl. Met. Mekh. Spl. Sredy* **17**(5), 91–100 (1986).

APPENDIX

The derivative $\nabla_k v_l$ of equation (6) is a twice covariant second-rank tensor component and is defined in the system (x^1, x^2). Its correlation with the Cartesian components of the same tensor is defined by [16]

$$\nabla_k v_l = (\nabla_\alpha v_\beta)\frac{\partial y_\alpha}{\partial x^k}\frac{\partial y_\beta}{\partial x^l}$$

where $\nabla_\alpha v_\beta$ means the usual derivative $\partial u_\beta/\partial y_\alpha$ in the Cartesian coordinate system (y_1, y_2). Then

$$g^{kl}\nabla_k v_l = \frac{\partial x^k}{\partial y_\gamma}\frac{\partial x^l}{\partial y_\gamma}\frac{\partial u_\beta}{\partial y_\alpha}\frac{\partial y_\alpha}{\partial x^k}\frac{\partial y_\beta}{\partial x^l} = \frac{\partial x^k}{\partial y_\beta}\frac{\partial u_\beta}{\partial x^k}$$
$$= \frac{\partial}{\partial x^k}\left[v_l\frac{\partial x^l}{\partial y_\beta}\left(\frac{\partial x^k}{\partial y_\beta}\right)_Q\right] = \frac{\partial}{\partial x^k}(\hat{g}^{kl}v_l) \qquad \text{(A1)}$$

where $\hat{g}^{kl}$ is defined according to equation (14).

The convective derivative $\nabla_k(v^k v_i)$ of equation (4) transforms as a twice covariant and once contravariant third-rank tensor

$$\nabla_k(v^k v_i) = \frac{\partial(u_\beta u_\gamma)}{\partial y_\alpha}\frac{\partial y_\alpha}{\partial x^k}\frac{\partial x^k}{\partial y_\beta}\frac{\partial y_\gamma}{\partial x^i}$$
$$= \frac{\partial(u_\beta u_\gamma)}{\partial x^k}\frac{\partial x^k}{\partial y_\beta}\frac{\partial y_\gamma}{\partial x^i}$$
$$= \frac{\partial}{\partial x^k}\left[u_\beta\left(\frac{\partial x^k}{\partial y_\beta}\right)_Q u_\gamma\left(\frac{\partial y_\gamma}{\partial x^i}\right)_Q\right]$$
$$= \frac{\partial(\hat{v}^k\hat{v}_i)}{\partial x^k} \qquad \text{(A2)}$$

where $\hat{v}_i$, $\hat{v}^k$ are defined according to equations (12) and (13).

The derivative $\nabla_k(\nabla_l v_i)$ in equation (4) transforms from one coordinate system into another as a three times covariant third-rank tensor. With equation (7) taken into account, the following equation is obtained:

$$g^{kl}\nabla_k(\nabla_l v_i) = \frac{\partial x^k}{\partial y_\delta}\frac{\partial x^l}{\partial y_\delta}\frac{\partial}{\partial y_\alpha}\left(\frac{\partial u_\gamma}{\partial y_\beta}\right)\frac{\partial y_\alpha}{\partial x^k}\frac{\partial y_\beta}{\partial x^l}\frac{\partial y_\gamma}{\partial x^i}$$

$$= \frac{\partial x^k}{\partial y_\beta} \frac{\partial}{\partial x^k} \left(\frac{\partial u_\gamma}{\partial x^l} \frac{\partial x^l}{\partial y_\beta} \right) \frac{\partial y_\gamma}{\partial x^i}$$

$$= \frac{\partial}{\partial x^k} \left(\hat{g}^{kl} \frac{\partial \hat{v}_i}{\partial x^l} \right) \quad \text{(A3)}$$

where $\hat{g}^{kl}$ is defined from expression (14).

The derivatives of equation (5) are transformed in an analogous way

$$\nabla_k (v^k \theta) = \frac{\partial (\hat{v}^k \theta)}{\partial x^k} \quad \text{(A4)}$$

$$g^{kl} \nabla_k (\nabla_l \theta) = \frac{\partial}{\partial x^k} \left(\hat{g}^{kl} \frac{\partial \theta}{\partial x^l} \right). \quad \text{(A5)}$$

CONVECTION NATURELLE VARIABLE DANS DES CAVITES PRISMATIQUES AVEC SECTION DROITE QUELCONQUE

Résumé—On étudie la convection naturelle bidimensionnelle, laminaire dans des cavités prismatiques horizontales de section droite quelconque. Avec l'approximation de Boussinesq, les équations de la convection sont écrites dans un système de coordonnées curvilinéaires non orthogonales et elles sont résolues par une méthode implicite aux différences finies. La convection naturelle variable est étudiée dans des régions quadrangulaires de configurations non conventionnelles : (a) un trapèze isocèle, (b) une portion de cercle entre deux cordes parallèles et égales, (c) une région limitée par une demi-onde cosinus et trois segments rectilignes. La solution des problèmes est obtenue dans le domaine de nombre de Grashof $10^2 \leqslant Gr \leqslant 10^6$ pour différents paramètres géométriques des cavités. On trouve que les valeurs maximales des fonctions de courant et du nombre de Nusselt peuvent subir des oscillations autour de leur valeur moyenne. Les résultats obtenus pour les cavités trapézoïdales sont en bon accord avec les données fournies par d'autres auteurs.

INSTATIONÄRE NATÜRLICHE KONVEKTION IN PRISMATISCHEN EINSCHLIESSUNGEN WILLKÜRLICHER GESTALT

Zusammenfassung—Die zweidimensionale laminare natürliche Konvektion in horizontalen prismatischen Einschlüssen willkürlicher Gestalt wird untersucht. Mit der Näherung von Boussinesq werden die Konvektionsgleichungen in einem körperangepaßten nicht-orthogonalen Koordinatensystem aufgestellt und mit einem impliziten Finite-Differenzen-Verfahren gelöst. Die instationäre natürliche Konvektion wird für viereckige Gebiete unüblicher Gestalt untersucht : (a) ein gleichschenkliges Trapez ; (b) ein Kreisausschnitt zwischen zwei gleichen parallelen Sehnen ; (c) ein Gebiet, dessen Berandungen eine Kosinus-Halbwelle und drei gerade Linien sind. Die Lösung wird für Grashof-Zahlen $10^2 \leqslant Gr \leqslant 10^6$ bei unterschiedlichen geometrischen Abmessungen der Einschließung hergeleitet. Es zeigt sich, daß die Maximalwerte der Stromfunktion und der Nusselt-Zahl den gedämpften Schwingungen um die stationären Werte zugeordnet werden können. Die Ergebnisse für die trapezförmigen Einschließungen stimmen gut mit Werten anderer Autoren überein.

НЕСТАЦИОНАРНАЯ ЕСТЕСТВЕННАЯ КОНВЕКЦИЯ В ПРИЗМАТИЧЕСКИХ ЕМКОСТЯХ ПРОИЗВОЛЬНОГО СЕЧЕНИЯ

Аннотация—Рассматривается двумерная ламинарная естественная конвекция в горизонтальных призматических емкостях произвольного поперечного сечения. Уравнения конвекции в приближении Буссинеска записываются в криволинейной неортогональной системе координат. Для решения уравнений используется неявный конечно-разностный метод. Исследована нестационарная естественная конвекция в четырехугольных областях нетрадиционной конфигурации: (а) область образована равнобочной трапецией; (в) область конвекции—часть круга, заключенная между двумя равными и параллельными хордами; (с) границы области образованы полуволной косинусоиды и тремя отрезками прямых линий. Решение задач найдено в диапазоне чисел Грасгофа $10^2 \leqslant Gr \leqslant 10^6$ при различных значениях геометрических параметров емкостей. Установлено, что максимальные значения функции тока и числа Нуссельта могут совершать затухающие колебания вблизи их стационарных величин. Результаты, полученные для трапецеидальных емкостей, хорошо согласуются с имеющимися данными других авторов.